



# Taper development when traverse grinding with diamond cup wheels

Jeffrey Badger (3)

*The Grinding Doc, Texas*

**Abstract:** Although cup wheels have been used in precision-grinding operations for over 100 years, little has been written about transient taper development in cup wheels and its significant effect on wheel wear, grinding heat, workpiece temperatures, size-holding, surface finish, cycle time, time between truing and machine-operator frustration. This article quantifies taper development and aggressiveness throughout the taper life-cycle. Wear profiles and grinding power are measured for four different production operations when grinding ceramic, cermets and tungsten-carbide with resin- and hybrid-bonded diamond wheels. Recommendations are made for coping with taper development, along with in-process truing considering recent developments in on-machine truing technology.

**Keywords:** grinding, diamond, cup-wheel

## 1. Introduction and background

Cup-wheel grinding has been used in mass production for over 100 years [1]. Today, it is used in precision grinding of tools, sawblades, gears, inserts and other components. In traverse cup-wheel grinding, the wheel is fed radially into the part at a fixed feedrate and a fixed axial depth of cut. For a new or freshly-trued wheel, all of the grinding action initially occurs on a small area on the outer-diameter wheel face. As a result, a taper develops on the wheel – first quickly and then more gradually – until finally encompassing the entire rim width.

This taper was first shown in 1914 by Guest [2], who showed a larger taper on the outer-diameter and a smaller taper on the inner-diameter (Figure 1). However, Guest did not elaborate on the cause of this taper or how it affected the grinding action. In the 108 years since, little has been written about taper development.

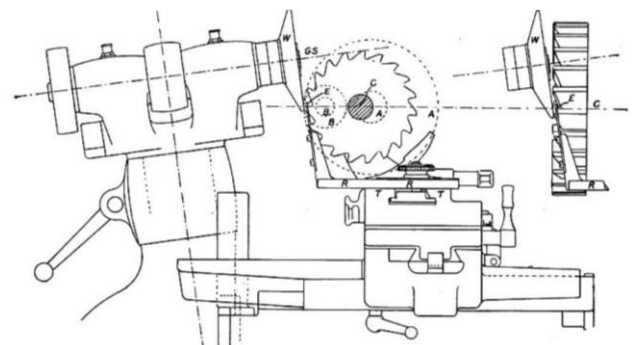
In production operations, this taper development has a large influence on heat generation, wheel wear and surface finish. The author has heard numerous anecdotes – particularly from sawblade and tool manufacturers – about how the grinding machine “grunts” after truing, following by “rumbling”, then steady-state “sweet spot” grinding, followed by “shrieking and screaming” and deterioration of the surface finish, at which point the operator retrues the wheel and begins the cycle again.

Therefore, this paper addresses taper development when traverse-grinding with cup wheels. It quantifies the aggressiveness as a function of the taper shape and how the changing aggressiveness leads to troublesome transient grinding behavior, including excessive heat generation, grinding forces, workpiece temperatures and wheel displacement along with workpiece surface-finish deterioration and longer cycle times.

## 2. Theory

### 2.1. Taper development and chip thickness

Numerous geometries of cup wheels exist – types 6A9, 11, 12, 11A9, 11A9, 11V9, 12A2, 12V2, etc. – and contain both conventional abrasives ( $\text{Al}_2\text{O}_3$ , SiC) and superabrasives (CBN, diamond) to grind almost all workpiece materials (steels, nickel alloys, tungsten-carbide, cermets, ceramics, PCBN, PCD, etc.).



Figs. 98 and 99. "Guest" Cutter Grinder. Diagram of Face Cutter Sharpening.

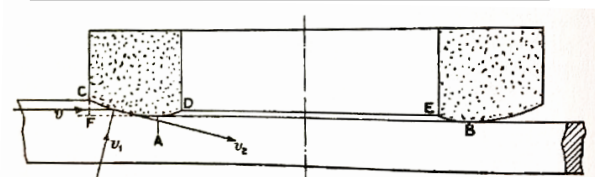


FIG. 24.—FEED IN CUP WHEEL WORK

**Figure 1.** Early work by Guest: 1903 [1] and 1914 [2].

Matsuo *et al.* [3] modelled the cross-sectional area of a theoretical chip assuming a sharp corner, akin to a 1A1 wheel. More recently, Gao *et al.* [4] modelled it as a taper and Badger *et al.* [5] modelled it as a taper with a flat. However, both of these assume a geometry that occurs only within a narrow, middle portion of the lifespan of the wheel.

### 2.2. Taper modelling

Prior to grinding, cup-wheels are typically: a) trued flat; or b) not trued at all, but simply mounted. The bottom rim of the cup-wheel begins as a flat surface, with a typical rim width of  $w_{\text{rim}}=2-8$  mm. When traverse grinding begins – with a depth of cut of  $a_e$  and a feedrate of  $v_w$  – almost all of the grinding action occurs on the outer-diameter of the wheel. The contact area is very small:  $A_{\text{cont}}=b_w \cdot a_e$ , where  $b_w$  is the workpiece width. As a result, the aggressiveness (and grit penetration depth, or chip thickness) is

enormous. Consequently, wheel wear is rapid and a taper quickly develops. Figure 2 illustrates the cup-wheel geometry both new and at some intermediate point after the taper has developed.

Assuming the depth of cut is kept constant, the height of the taper will be close to the depth of cut, i.e.,  $h_{taper} \cong a_e$ . This creates two regions on the wheel: 1) the roughing region, where wheel-workpiece contact occurs along the taper,  $l_{taper}$ ; and b) the finishing region, where wheel-workpiece contact occurs along the flat width,  $w_{flat}$ , at a theoretical depth of cut of zero. The roughing region removes almost all of the material, and the finishing region produces a better surface finish. The wheel-workpiece contact area for a new wheel is  $A_{cont}=a_e \cdot b_w$ . For a tapered wheel, it is  $A_{cont}=l_{taper} \cdot b_w$ , where  $l_{taper}=\sqrt{(h_{taper}^2+W_{taper}^2)}$ .

The *Aggressiveness Number* [6] is a dimensionless term that quantifies how aggressively the grits are attacking the workpiece. It is proportional to chip thickness or grit penetration depth but circumvents the problem of having to quantify the grinding-wheel topography [6]. Larger values typically produce greater wheel wear, rougher surface finishes and lower specific grinding energies. On the taper, it is defined as [7]:

$$Aggr = 10^6 \cdot v_w \cdot \sin(\alpha) / v_s \quad (1)$$

where  $\alpha$  is the taper angle and  $v_s$  is the wheel surface speed. For a straight taper, the taper angle is defined according to  $\tan(\alpha) = h_{taper}/W_{taper}$ , although it can vary along the taper geometry. It is valid for both pre-taper ( $\alpha=90^\circ$ ) and post-taper ( $90^\circ > \alpha > 0^\circ$ ) [7].

To illustrate, we can take some typical parameters when grinding tungsten-carbide-tipped sawblades with a resin-bonded diamond wheel when the taper is at an intermediate state ( $W_{taper} = \frac{1}{2} \cdot W_{rim}$ ):  $a_e=0.050$  mm,  $d_s=125$  mm,  $v_w=50$  mm/s;  $v_w=20$  m/s,  $b_w=3$  mm,  $W_{rim}=6$  mm and  $W_{taper}=3$  mm, yielding  $Q'=a_e \cdot v_w=2.5$  mm<sup>2</sup>/s.

The wheel-workpiece contact areas and Aggressiveness Numbers are given in Table 1.

**Table 1.** Contact area, aggressiveness and grit penetration depth before and after full taper development.

	<u><math>A_{cont}</math></u>	<u><math>Aggr</math></u>	<u><math>GPD</math></u>
before taper	0.15 mm <sup>2</sup>	2500	7.1 μm
after taper	9.0 mm <sup>2</sup>	42	0.9 μm

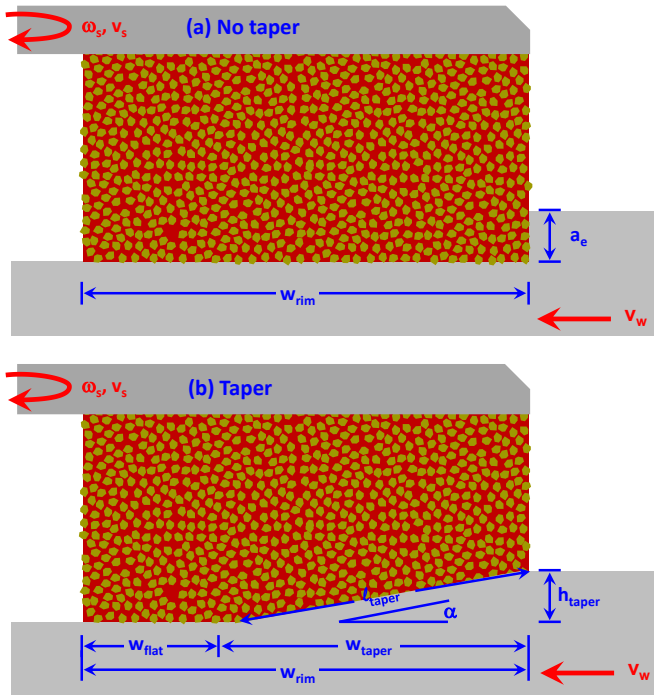


**Figure 2.** Taper development.

Upon development of the taper, the contact area has increased drastically: from 0.15 mm<sup>2</sup> to 9.0 mm<sup>2</sup>, a factor of 60X. This drastically reduces the aggressiveness, from  $Aggr=2500$  to  $Aggr=42$ , also a factor of 60X.

We can also quantify the operation in terms of the grit penetration depth,  $GPD$ . Here some assumptions need to be made, namely the cutting point density,  $C$ , and the ratio of chip width to chip height,  $R$ . Values can be pulled from Malkin's measurements [8] when grinding tungsten-carbide with a 140/170-mesh resin-bonded diamond wheel:  $C=5$  points/mm<sup>2</sup> and  $R=20$ . Using the formula for grit penetration depth in face grinding [7], this gives a value of  $GPD=7.1$  μm before taper development and 0.9 μm after taper development. Again, the difference is huge, and two very different grinding scenarios will develop for these two different conditions. In fact, when the taper is fully developed and reaches some steady-state value ( $W_{taper}=W_{rim}=6$  mm), the grit penetration depth decreases even further, to  $GPD=0.6$  μm.

### 2.3. Single-doink vs. double-doink

During most traverse cup-wheel grinding operations, the in-feed is done one of three ways: 1) Before the forward pass, with no zero-in-feed "sparkout" pass (referred to colloquially as *single-doink grinding*); 2) Before the forward pass, with a zero-in-feed sparkout pass (*single-doink + sparkout grinding*); or, 3) Before the forward pass and again before the reverse pass (*double-doink grinding*).

The tapers that develop for these three scenarios are very different. They are illustrated in Figure 3. A fourth type can also occur, when both sides of the wheel traverse completely through the part. In this case, the taper that develops is similar to that in *single-doink + sparkout*.

### 2.4. Finishing "sparkout" revolutions

One of the benefits of having a longer "sparkout" flat width,  $w_{flat}$ , is that it produces a better surface finish (i.e., a lower  $R_a$ ). The number of zero-depth finishing revolutions of the grinding wheel,  $N_{fin}$ , can be quantified as:

$$N_{fin} = w_{flat} \cdot RPM_s / v_w \quad (2)$$

where  $RPM_s$  is the angular velocity of the grinding wheel in revolutions per minute. In the example above ( $RPM_s=3056$  RPM,  $w_{rim}=6$  mm), the no-taper wheel ( $w_{flat} = 6$  mm) produces 6 finishing wheel revolutions and the tapered wheel ( $w_{flat}=3$  mm) produces 3 finishing wheel revolutions. When the taper is fully developed ( $W_{taper} \sim W_{rim}=6$  mm,  $w_{flat} \sim 0$  mm), the number of finishing wheel revolutions decreases to  $N_{fin} \sim 0$  and the surface finish deteriorates. At this point the operator either stops the operation to retrue the wheel or slows down the feedrate to improve surface finish.

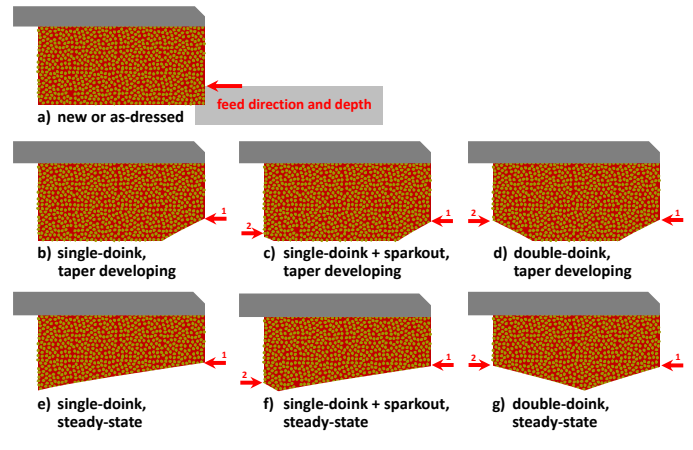


**Figure 3.** Taper development in single-doink and double-doink.

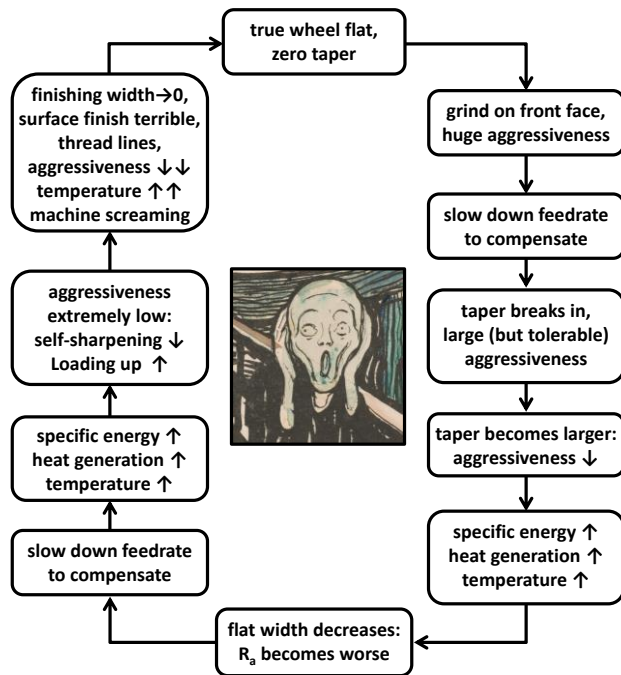


Figure 4. The Taper Cycle of Madness.

### 2.5. The Taper Cycle of Madness

After mounting a new wheel or after truing, the huge aggressiveness experienced by the outer-diameter wheel face is often accompanied by an unpleasant grunting sound as layers of diamond grits are quickly ripped out of the bond material. In addition, the workpiece – for example, a carbide-tipped sawblade – runs the risk of edge-chipping owing to the deep penetration of the diamonds or of the tip shearing off at the point of brazing.

To remedy this, operators often slow down the feedrate. This does reduce the chipping-risk (as aggressiveness decreases), but also results in a longer cycle time. In addition, as the taper lengthens, if the feedrate is not increased proportionally, the aggressiveness will decrease significantly, resulting in higher specific energies, greater heat generation, higher workpiece temperatures, larger normal forces, larger wheel deflection, greater loading and poorer wheel self-sharpening [9].

As the taper length increases and eventually approaches the rim width, the aggressiveness becomes extremely small. Grinding power is high, wheel loading (and, in some materials, diamond dulling) can become severe, and workpiece breakage or chipping can occur. In addition, the surface finish steadily becomes worse as the number of finishing revolutions decreases, eventually approaching zero. Often, audible grunting or screaming sounds can be heard emanating from the grinding machine.

To remedy this, operators often take action, which can involve truing the wheel (costing time and beginning the cycle again), decreasing the depth of cut, sticking the wheel (to remove loading), or slowing down the feedrate (to reduce the material removal rate and increase the number of finishing revolutions).

Slowing down the feedrate can be the most detrimental. The benefit of the lower  $Q'$  associated with the slower feedrate is rapidly offset by the larger specific energy, poorer wheel self-sharpening and longer time in the hot zone. This was shown by work done on grinding of cermet [5], where specific energies increased from  $e=500 \text{ J/mm}^3$  to  $e=1900 \text{ J/mm}^3$  simply by decreasing the feedrate by 75%.

Using a Jaeger-based model of grinding temperature [10,11] –  $T_{wp} \propto P_g/A_{cont} \cdot \sqrt{t_{hz}}$ ;  $t_{hz} = w_{taper}/v_w$ ;  $P_g = e \cdot Q$  – where  $T_{wp}$  is the increase in workpiece temperature,  $P_g$  is the grinding power and  $t_{hz}$  is the time in the hot zone, this 75% reduction in feedrate would actually increase workpiece temperature by 90%. And yet, that is often the first action taken by operators when problems occur.

The other action taken by operators is simply to true the wheel and begin the *Taper Cycle of Madness* all over again. This cycle is illustrated in Figure 4.

### 2.6. Quantification of The Cycle of Madness

This cycle can be quantified. The aggressiveness and number of finishing revolutions as the taper gradually breaks in are shown in Figure 5. The operator initially chooses a feedrate (here  $v_w=10 \text{ mm/s}$ ) to give a reasonable value of  $Q'=0.05 \text{ mm}^2/\text{s}$ . Upon commencement of grinding with the huge aggressiveness, the operator hears the grunting sound or is concerned with chipping and tip breakage and slows down the feedrate by a factor of 10, reducing the removal rate to a low  $Q'=0.005 \text{ mm}^2/\text{s}$  but producing a large but tolerable value of  $Aggr=50$ . Grinding now begins, albeit with a longer cycle time.

The taper then develops, quickly reducing the aggressiveness to, say,  $Aggr=5$  at a taper width of  $w_{taper}=0.5 \text{ mm}$ . This increases the amount of rubbing and heat generation. Eventually, the taper encompasses the entire rim width,  $w_{taper} \sim w_{rim}=6 \text{ mm}$  and the aggressiveness has decreased by a factor of 120, resulting in an enormous amount of rubbing and heat generation and a greater risk of temperature-induced workpiece cracking. In spite of the low aggressiveness, wheel wear can also be high due to temperature-induced resin degradation [9]. The flat width has now approached zero,  $w_{flat} \sim 0 \text{ mm}$ , and surface finish has deteriorated. At this point the operator decides to retrue the wheel – and begin anew the *Taper Cycle of Madness*.

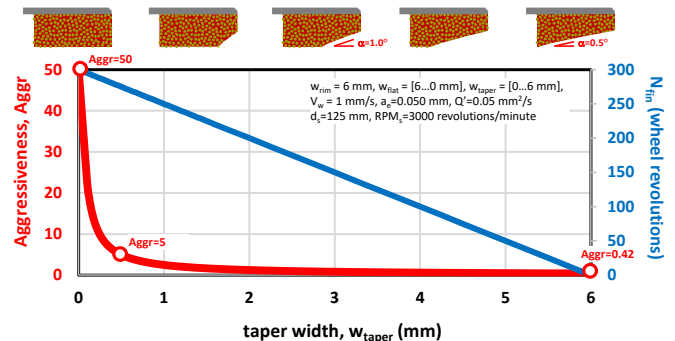


Figure 5. Effect of taper development on key outputs.

## 3. Experimental and results

Data was collected during visits to several production companies using resin- and hybrid-bonded diamond cup wheels to grind: 1) advanced ceramics for the semiconductor industry, 2) cermet-tipped sawblades, 3) tungsten-carbide-tipped sawblades, and 4) tungsten-carbide round tools. These are each taken individually, with a focus on taper development and how it affected grinding.

### 3.1. Vertical-spindle surface grinding of ceramics

During a visit to a company performing vertical-spindle spiral-traverse surface grinding of ceramics with a resin-bonded diamond cup wheel ( $d_s=76.2 \text{ mm}$ ,  $w_{rim}=6 \text{ mm}$ ,  $v_w=2.54 \text{ mm/s}$ ;  $v_s=19.2 \text{ m/s}$ ,  $a_e=0.508 \text{ mm}$ ,  $CF=15.24 \text{ mm}$ , described in [7]), the shape of the taper was measured at various times over the course of several days by plunging the wheel axially into a thin piece of

graphite ( $w=3$  mm) mounted in a vice. A photograph was taken and the shape was transferred into a graphics software.

Geometrically, the grinding action before taper break-in is akin to cylindrical grinding, with: a) the depth of cut equal to the cross-feed ( $a_e=CF=15.24$  mm); b) the contact width equal to the depth of cut ( $b_s=a_e=0.508$  mm); and c) the feedrate equal to the circumferential workpiece velocity ( $v_w=2.54$  mm/s). Consequently, these parameters produce an obscenely high specific material removal rate of  $Q'=38.7$  mm<sup>2</sup>/s (whereas typical values in ceramics might be  $Q'=1$  mm<sup>2</sup>/s), creating a huge aggressiveness on the outer-diameter before a taper breaks in.

Power measurements were made during grinding, with a typical value of 1.5 kW. Considering the wheel speed of  $v_s=19.2$  m/s and assuming a conservative ratio of normal force to tangential force of  $F_N/F_T = 4.0$  [12], this produces an estimated normal force of  $F_N=310$  N ( $P=F_T \cdot v_s$ ). A measurement was made of the axial spindle stiffness by pushing up on the spindle with a constant force and measuring the displacement, yielding a stiffness of 39 N/ $\mu$ m. Considering this, a rough estimate of the upward (axial) spindle deflection is 8  $\mu$ m.

Considering how these variables may affect the development of the taper, the shapes of the various measured tapers can be examined. This is shown in Figure 6.

Taper (a) was taken shortly after the wheel had been mounted. Here a short taper can be seen. The taper height, as expected, is close to the depth of cut. The taper angle is approximately  $\alpha=\text{atan}(h_{\text{taper}}/w_{\text{taper}})=20^\circ$ . In addition, it can be seen that the inside-diameter of the wheel is developing a small taper where the wheel reengages the workpiece.

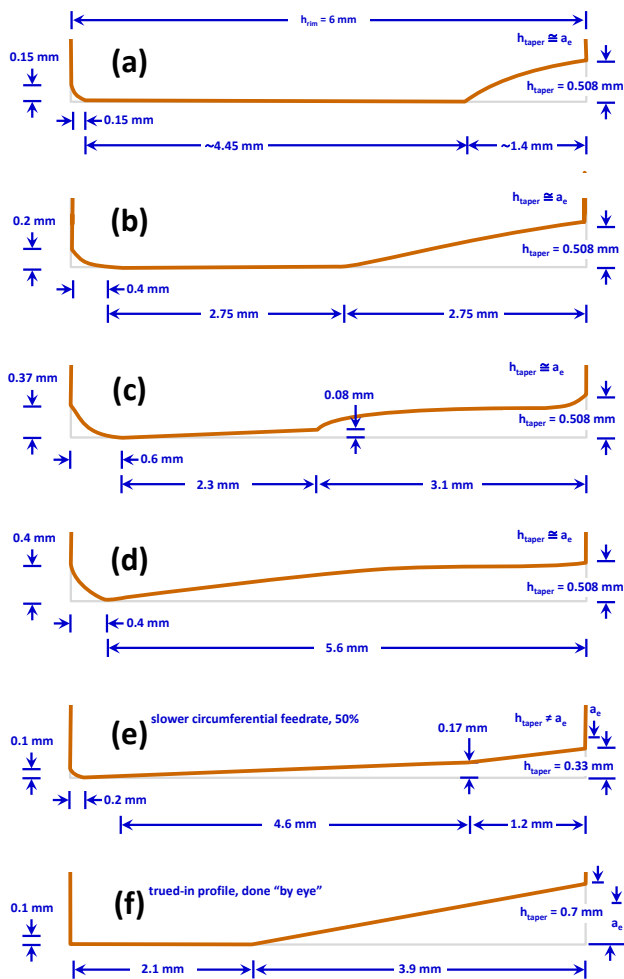


Figure 6. Measured tapers.

Taper (b) was measured after the wheel had ground more ceramic material. Here approximately half of the wheel is rough-grinding and half is finish-grinding. Depending on the parameters chosen, this could be seen as the optimum geometry: enough taper to do the roughing with a sweet-spot aggressiveness, enough finishing width to give a good surface finish.

Taper (c) starts to deviate from the standard straight line. Here the other factors must be considered, in particular the larger deflection due to the larger normal force associated with the smaller aggressiveness and possible loading and diamond-dulling.

Taper (d) shows a wheel that has developed a taper that encompasses almost the entire rim width. Here, the finishing width is approaching zero. Typically, this is the point where many operators will retrue the wheel as the surface finish will have deteriorated. In addition, the taper length is so long that values of aggressiveness will be small, resulting in large specific energies and, in turn, large grinding power and large normal forces.

Taper (e) developed after a change in grinding parameters: a 50% reduction in workpiece velocity and a 50% reduction in depth of cut. This illustrates the perils of changing the depth of cut. When the depth of cut is decreased after the taper has already fully formed, the grinding action occurs on a fraction of the taper length. Here, a secondary taper will develop at a smaller angle, as seen in the figure. Wheel wear will continue to occur until the previous taper is worn away.

Taper (f) is not a naturally-worn taper. Rather, the operators decided to true in a taper on the machine. Typically, diamond wheels are trued with  $\text{Al}_2\text{O}_3$  or SiC wheels via a motor-driven or brake-controlled dresser. In this case, neither was available. Instead, a 75-mm-diameter, 25-mm-wide, 60-mesh, I-grade  $\text{Al}_2\text{O}_3$  wheel was mounted in a vice inside the guarded machine and the cup wheel was traversed back and forth radially until a flat was developed. Then the wheel was traversed at an angle to create the taper. A taper angle was chosen to produce a flat width of half the rim width ( $w_{\text{flat}}=1/2 \cdot w_{\text{rim}}$ ) and a taper height the same as the depth of cut ( $h_{\text{taper}}=a_e$ ), or:  $\alpha=\text{atan}(a_e/w_{\text{taper}}) = 0.508/3 = 9.6^\circ$ .

Since the removal depth to reach a 3 mm flat width was unknown, the operators had to "eyeball" the wheel at a distance, arriving at the final profile as shown, leading to a slightly shorter flat width and higher taper width than calculated. Nevertheless, this grinding operation would commence at a known aggressiveness value and a known flat width.

### 3.2. Cermet grinding

During a visit to a European company grinding cermet-tipped sawblades with a resin-bonded d107 diamond wheel ( $v_s=20$  m/s;  $v_w=1$  mm/s;  $a_e=0.05$  mm,  $b_{\text{rim}}=2$  mm,  $b_w=2.4$  mm), the grinding power was measured and then converted to specific energy ( $e=P/Q$ ,  $Q=a_e \cdot v_w \cdot b_w$ ). Higher values of specific energy indicate more rubbing and less cutting, often caused by low aggressiveness values, dull grits, and/or a loaded wheel.

Cermets are considered much more difficult to grind than tungsten-carbide owing to the hard particulates that cause diamond dulling [5]. This results in larger specific energies and greater wheel wear. When grinding cermets, typical values of specific material removal rate are in the range of  $Q'=0.3-0.5$  mm<sup>2</sup>/s [13,14,5]. The company here was grinding at  $Q'=0.05$  mm<sup>2</sup>/s.

Values of specific energies when grinding cermets are typically in the range of 100-500 J/mm<sup>3</sup> [5,13,14]. For the company in the example, the measured value was 1670 J/mm<sup>3</sup>.

This leads to the question of why the company was grinding at such a low  $Q'$ , producing huge specific energies and longer cycle times. The answer may lie in the *Taper Cycle of Madness*. In the case here, a freshly trued wheel grinding at a feedrate of  $v_w=8$  mm/s

(chosen to achieve a respectable specific removal rate for cermets of  $Q'=0.4 \text{ mm}^2/\text{s}$ ) would be grinding at  $\text{Aggr}=400$ , a huge value.

This would likely produce a grunting sound along with a large shearing force acting on the carbide tip, increasing the risk of tooth breakage and chipping. To remedy this, the operator may have slowed down to the  $v_w=1 \text{ mm/s}$  feedrate, producing a large but not ridiculous value of  $\text{Aggr}=50$ , as shown in Figure 7.

This value is reasonable for a freshly trued wheel. However, it is not reasonable once the taper starts to break in. This is shown in the figure. Measured values from the Inasaki tests are given, showing values of aggressiveness ranging from 5 to 60 for a similar diamond-grit size, in line with the initial value of  $\text{Aggr}=50$  for the freshly trued wheel with the slow feedrate.

However, as the taper develops, the aggressiveness decreases, eventually reaching a value of  $\text{Aggr}=1.25$  when the taper is fully developed ( $w_{\text{taper}}=w_{\text{rim}}=2 \text{ mm}$ ). This forty-fold decrease causes excessive rubbing and poor diamond-self-sharpening, excessive wheel leading, huge specific energies, large normal forces and often the screaming sound. The operator then trues the wheel to begin the cycle again and escape the dangerously large specific energy value of  $e=1670 \text{ J/mm}^3$ .

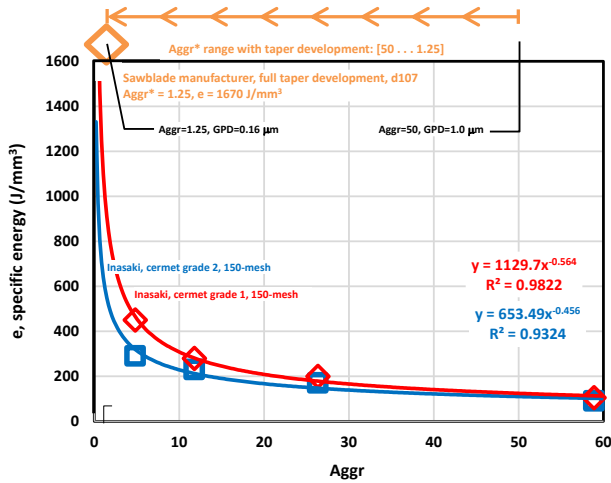


Figure 7. Aggressiveness and specific energy in cermet grinding.

### 3.3. Natural wear profile – tri-grit wheels

During a visit to a company sharpening tungsten-carbide-tipped sawblades, a measurement was made of the taper shape on a worn, resin-bonded diamond cup wheel at 13 points along the 6-mm-wide rim width. The wheel was a tri-grit “sandwich” wheel with three different mesh sizes: 150M, 400M and 1200M, as shown in Figure 8. The wheel had been grinding several days without truing.

In general, larger grits give less wheel wear whereas smaller grits tend to produce a finer (lower  $R_a$ ) surface finish. It is assumed that the tri-grit wheel was designed such that the final removal would be done by the finer grits, producing a better surface finish.

The figure appears to show that the real advantage may be in that the smaller, 1200-mesh diamonds wear away so quickly that a flat is developed and, more importantly, maintained – even when the wheel had reached steady-state wear conditions. In this sense, retrueing is not necessary to restore the flat width to maintain a good surface finish. Rather, the flat width is maintained during steady-state conditions. In this sense, the tri-grit wheel avoids the *Taper Cycle of Madness*.

### 3.4. Changing profile – tool grinding

A collaboration was made with a large German machine-tool builder. Tungsten-carbide round tools were ground with a hybrid-bonded d46 diamond cup wheel:  $v_s=22 \text{ m/s}$ ;  $v_{tr}=40 \text{ mm/min}$ ,

$b_{\text{rim}}=3 \text{ mm}$ , cup-wheel angle  $\beta=20^\circ$ ,  $a_e=0.4 \text{ mm} \times 50 \text{ passes}$ ,  $a_c=20 \text{ mm}$ ,  $d_w=12 \text{ mm}$ ,  $d_s=100 \text{ mm}$ , oil coolant. The grinding power was measured and then converted to specific energy ( $e=P/Q$ ). The cup-wheel profile was measured both after truing (orange) and after grinding (red). Figure 9 shows the change in taper geometry and the increase in power, owing to: a) the changing aggressiveness, and b) wheel loading.

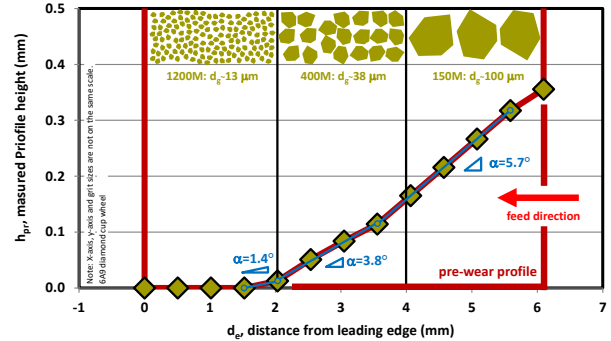


Figure 8. Measured profile height of tri-grit wheel.

## 4. Discussion

The results show that the transient behavior of tapers in cup-wheel grinding has a significant effect on aggressiveness and, in turn, grinding power and heat generation, wheel wear, diamond-dulling, surface finish and cycle times. The situation appears to be worse in cermet grinding than in tungsten-carbide grinding, where grit-dulling is more of a problem.

The two extremes of taper development – no taper and all taper with no flat width – each cause significant but different problems in the grinding operation. The degree of these extremes depends on the range of aggressiveness during taper development. If we assume that at full taper  $w_{\text{taper}} \cong w_{\text{rim}}$ , the ratio of initial aggressiveness to final aggressiveness reduces to  $\text{Aggr}_i/\text{Aggr}_f \sim w_{\text{rim}}/a_e$ . In the example above when grinding ceramics with a large depth of cut and a slow feedrate, the ratio was  $\text{Aggr}_i/\text{Aggr}_f \sim 6/0.508=11.8X$ . This could be considered in the slow-&-deep regime. In contrast, in the cermet-grinding example, the small depth of cut and fast feedrate resulted in a ratio of  $\text{Aggr}_i/\text{Aggr}_f \sim 6/0.05=120X$ . This could be considered in the fast-&-shallow regime. Owing to the larger values of  $\text{Aggr}_i/\text{Aggr}_f$ , grinding operations in the fast-&-shallow regime will suffer more from the *Taper Cycle of Madness*.

One solution is to increase the feedrate (or decrease the wheel speed) as the taper develops. In theory, this is reasonable and operators do this. However, the rate of taper development is not easy to predict or measure, especially considering that the operator may be responsible for several machines at once, all with different tapers and different rates of taper development.

Another option is to monitor power. Figures 7 and 9 show that power increases as the taper changes, the wheel loads and the grits dull. This information about the change in power could be used to make changes to the feedrate to compensate for the increasing taper. While taper measurements are time-consuming and not all machines are capable of in-process measurements, almost all modern machines have the capability of monitoring power.

Another practical approach is simply to use a tri-grit wheel. Figure 8 shows that the benefit is not necessarily in the smaller grits, but in the flat that develops during steady-state wear. This method appears to be quite robust as it does not require any operator intervention. However, care must be taken as a reverse sparkout pass may cause the small-grit area to wear away, eliminating any benefit. In addition, since the benefit appears to

come predominantly from the flat development, a single-mesh wheel of differing hardness could also achieve the same function.

Another approach is to simply have the machine measure the taper periodically throughout the cycle and make adjustments to the feedrates. Twenty years ago, this would not have been possible. Nowadays, with probes measuring sawblade heights and making adjustments to account for wheel wear, in-process measurement of the rim geometry should also be possible.

However, even this method will result in a steady-state geometry with near-zero flat width. One solution is to true the wheel in the machine. More and more machines now have this capability. When the flat width becomes smaller than, say, 1 mm, the wheel could be automatically trued back to  $w_{flat}=2$  mm and a taper angle trued to give a taper height the same as the depth of cut. One challenge would be knowing how many passes are required to create the geometry. However, recent advances in truing of diamond wheels [15], including typical D-ratios (the volume of  $Al_2O_3/SiC$  abrasive required to remove unit volume of diamond wheel), would be helpful in estimating these values. In addition, truing would enable the grinding operation to avoid the “chunky wear” regime that eventually results after the collapse stage of the wheel [16], where the unround wheel produces intermittent contact, greater wheel wear and possible “snakeskin chatter” marks on the wheel [17].

Finally, simply being aware of this taper development may be enough for many machine operators to make the necessary adjustments. The author has visited numerous companies using cup wheels. Simply making operators and engineers aware of the concept of taper development has allowed them to make their own decisions on a case-by-case basis. Knowing is half the battle.

- Before this taper develops, grinding is performed on the outer-diameter face with an extremely large aggressiveness.
- As this taper gradually develops, the aggressiveness decreases. This results in larger specific energies, larger normal forces, greater spindle deflection, less wheel self-sharpening, more diamond-grit dulling and greater wheel loading. At full taper development, specific energies can become huge.
- As the taper gradually develops, the flat width decreases, resulting in fewer finishing revolutions and a rougher surface finish ( $R_a$ ).
- At full taper, the wheel is often retrued to reduce heat generation and improve surface finish.
- This ever-changing taper followed by retruing is known as the *Taper Cycle of Madness*.
- The *Taper Cycle of Madness* is more pronounced in fast-&-shallow grinding operations compared to slow-&-deep grinding operations, when the value of  $w_{rim}/a_e$  is smaller.
- Tri-grit wheels can be useful in maintaining a steady-state flat on the wheel, avoiding the *Taper Cycle of Madness*.
- Truing a taper and a flat onto the wheel can be beneficial in maintaining consistent grinding action, staying in the sweet-spot of the wheel and maintaining a consistent finishing flat width.
- It is recommended that machine builders incorporate even simple truing in their machines to maintain a near-constant taper geometry. This would result in larger material-removal rates, shorter cycle times, less wheel consumption and better and more consistent surface finishes.

## Funding and Acknowledgements

This project was funded independently by Dr. Jeffrey A. Badger. He would like to thank Tim Cook at Cook’s Resharpener in Texas and Jürgen Hauger at Vollmer Maschinenfabrik in Biberach, Germany.

## References

- Hodgson, Richard Broom (1903) *Emery Grinding Machinery*. Section by Guest.
- Guest JJ (1914) *Grinding Machinery*. London: Edward Arnold.
- Matsuo T, Touge M, Yamada H (1997) High-precision surface grinding of ceramics with superfine grind diamond cup wheels. *CIRP Annals*, **46**/1:249-252.
- Gao B, Bao W, Jin T, Chen C (2021) Variation of wheel-work contact geometry and temperature responses: Thermal modeling of cup wheel grinding. *International Journal of Mechanical Sciences*, **196**:1-15.
- Badger J, Dražumerič R, Krajnik P (2016) Grinding of cermets with cup-wheels. *Materials Science Forum*, **874**:115-123.
- Dražumerič R, Badger J, Roininen R, Krajnik P (2020) On geometry and kinematics of abrasive processes: The theory of aggressiveness. *International Journal of Machine Tools & Manufacture* **154**:1-13.
- Badger J, Dražumerič R, Krajnik P (2021) Application of the dimensionless Aggressiveness number in abrasive processes. *Procedia CIRP*, **102**:361-368.
- Zelwer O, Malkin S (1980) Grinding of WC-Co cemented carbides. *ASME Journal of Engineering for Industry* **102**:133-139.
- Badger J (2015) Grinding of sub-micron-grade carbide: Contact and wear mechanisms, loading, conditioning, scrubbing and resin-bond degradation. *CIRP Annals*, **64**:341-344.
- Jaeger JC (1942) Moving sources of Heat and the Temperature at Sliding Contacts. *Proceedings of the Royal Society of New South Wales*, **76**:203-224.
- Malkin S, Guo C (2008) *Grinding Technology: Theory and Applications of Machining with Abrasives, Second Edition*, Industrial Press, Inc.
- Liao TW, Li K, McSpadden SB (2000) Wear mechanisms of diamond abrasives during transition and steady stages in creep-feed grinding of structural ceramics. *Wear* **242**:28-37.
- Kumar C (1995) Grinding of Cermet Tool Materials. *Proc. of the SuperGrind Conference*, 69-78.
- Toyama I, Inasaki I, Shiratori H (1993) High Efficiency Grinding of Cermet. *Japan Society for Mechanical Engineers*, **59**: 267-272.
- Dražumerič R, Badger J, Klement U, Krajnik P (2018) Truing of diamond wheels—Geometry, kinematics and removal mechanisms. *CIRP Annals*, **67**/1:345-348.
- Badger J (2009) Factors affecting wheel collapse in grinding. *CIRP Annals*, **58**/1:307-310.
- Hahn R, Lindsay R (1971) *Principles of Grinding Part V: Grinding chatter, in Principles of Grinding: Theory, Techniques and Troubleshooting*, Editor: Bhatteja CL, Society of Manufacturing Engineers.

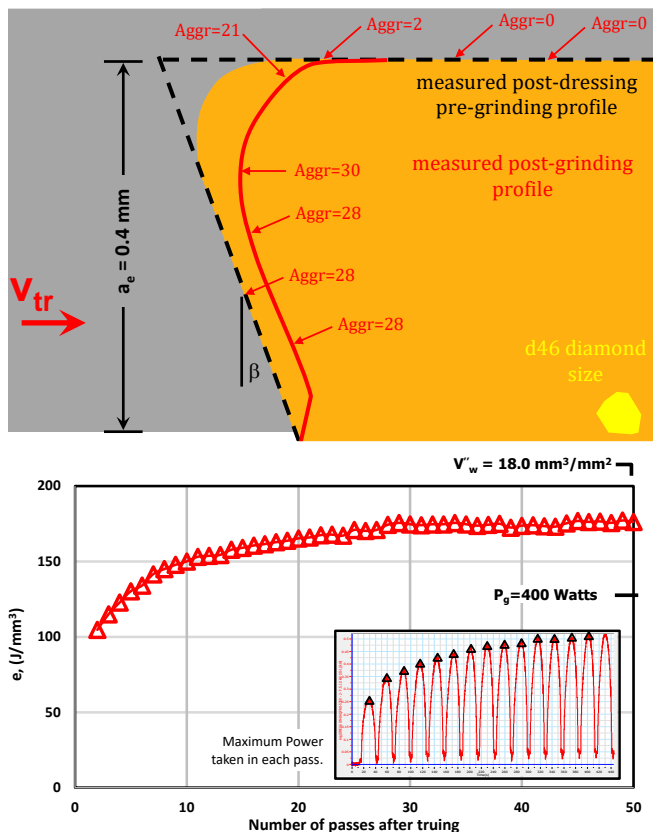


Figure 9. (top) Cup-wheel profile and (bottom) grinding power.

## 5. Conclusions

- During traverse-grinding with cup wheels, a taper gradually develops on the bottom rim face of the wheel.